Impact of photon recycling on the light extraction from metal halide perovskite light emitting diodes

Urs Aeberhard[1] · **Simon J. Zeder[1]** · **Beat Ruhstaller[2]**

Abstract

The impact of photon recycling on the efficiency of light extraction from metal halide perovskite light emitting diodes is quantified using a novel modelling framework based on a detailed-balance compatible Green dyad approach. Analysis of photon modes contributing to internal emission and iterative evaluation of re-absorption and re-emission processes is performed for single perovskite layers in absence and presence of a metallic reflector and under consideration of associated parasitic absorption losses. Finally, the approach is employed to characterize the emission characteristics of a realistic multilayer device stack in dependence of the emitter thickness.

1 Introduction

In the last decade, metal halide perovskites have emerged as a class of materials that can be used to engineer efficient light-emitting devices (Tan et al. 2014; Stranks and Snaith 2015; Zhang et al. 2017). In high quality metal halide perovskite materials, strong optical absorption with sharp onset together with low non-radiative charge carrier recombination rates leads to the presence of sizable photon recycling (PR) effects, which can improve light extraction

✉ Beat Ruhstaller
beat.ruhstaller@zhaw.ch

Urs Aeberhard
urs.aeberhard@fluxim.com

Simon J. Zeder
simon.zeder@fluxim.com

[1] Fluxim AG, Winterthur, Switzerland

[2] ZHAW - Zurich University of Applied Sciences, Winterthur, Switzerland

from perovskite LEDs due to redistribution of light from guided to out-coupled modes (Cho et al. 2020).

In order to exploit the beneficial impact of PR in perovskite LEDs (PeLEDs), accurate quantification of internal and external emission in dependence of the multilayer stack design is required. Recently, a simulation approach based on a transfer-matrix dipole model was presented (Cho et al. 2020; Cho and Greenham 2021), which allows for a comprehensive analysis of the photon modes contributing to internal emission and to both, recycling and parasitic absorption of the internally emitted photons. However, the approach suffers from two important limitations: First, in order to avoid divergencies in the dissipated power related to non-radiative near-field energy transfer, it demands a discrete partitioning of the system to create a non-absorbing environment of the dipole source at a given location, as well as selection of an in-plane wave vector cut-off, which are both origin of inaccuracies and introduce some arbitrariness in the solution. Second, the approach is purely optical, and, hence, does not allow for the consideration of aspects of electronic transport and non-radiative losses related to a specific device stack design.

We therefore introduced a theoretical treatment of photon emission and recycling in opto-electronic semiconductor devices that is not only free of non-physical divergencies, but also compatible with detailed balance, and which provides the internal and external emission in terms of the local values of optical constants and quasi-Fermi level splitting (QFLS) and of the transverse electromagnetic Green's dyad (Aeberhard et al. 2021). In this way, it enables seamless integration with opto-electronic device simulation tools that use the radiative recombination and secondary photogeneration rates in the charge carrier balance equations and provide an update of the local QFLS to be used in the computation of those rates.

Here, we now show the application of this framework to the assessment of the impact of PR on the light extraction efficiency in PeLED components and devices, from the analysis of contributing photonic modes in single emitter slab configurations to the evaluation of the external LED quantum efficiency in realistic device stacks.

2 Theoretical model

This section summarizes the main components of the theoretical description of photon recycling based on dyadic Green's functions as derived recently (Aeberhard et al. 2021). It also discusses the formal analysis of the light out-coupling efficiency based on the contributions of different optical modes to internal and external emission. Finally, the role of the quasi-Fermi level splitting is investigated in the limits of ideal transport and of full carrier localization.

2.1 Light emission and re-absorption from dyadic Green's functions

The theoretical formalism on which the modelling approach is based merges the theory of dipole emission in semiconductor multilayers (Paulus et al. 2000) with a local quasi-equilibrium approximation of the non-equilibrium Green's function (NEGF) framework for the quantum kinetics of excited semiconductors, which was shown to provide a consistent theory of absorption and emission at the sub-wavelength regime (Aeberhard and Rau 2017). This provides an expression of the Poynting vector as a function of the local optical material constants (refractive index n_r and extinction coefficient κ), the local QFLS $\Delta\mu_{cv}$ and the dyadic Green's function $\overleftrightarrow{G}$ of the transverse fields, e.g. for the TE component:

$$S_z^y(z, E_\gamma) = \frac{4E_\gamma^3}{\hbar^3 c_0^2 \pi} \int dz' \left\{ n_r(z', E_\gamma) \kappa(z', E_\gamma) f_{BE}\left(E_\gamma - \Delta\mu_{cv}(z')\right) \right.$$

$$\left. \times \Im \int \frac{d^2 q_\parallel}{(2\pi)^2} G_{yy}(\mathbf{q}_\parallel, z, z', E_\gamma) \left[\partial_z G_{yy}(\mathbf{q}_\parallel, z, z', E_\gamma)\right]^* \right\} \tag{1}$$

where z is the perpendicular position, E_γ the photon energy, $q_\parallel$ denotes the in-plane photon wave vector and f_{BE} is the Bose-Einstein distribution function. While this expression provides the external emission, the internal emission is given by a generalization of the Van Roosbroeck-Shockley (VRS) relation to arbitrary local photon density of states:

$$\mathcal{R}_{em}(z, E_\gamma) = \frac{4E_\gamma^2}{\hbar^3 c_0^2 \pi} n_r(z, E_\gamma) \kappa(z, E_\gamma) f_{BE}\left[E_\gamma - \Delta\mu_{cv}(z)\right]$$

$$\times \Im \left\{ \sum_{\mu=x,y,z} \int \frac{d^2 q_\parallel}{(2\pi)^2} G_{\mu\mu}(\mathbf{q}_\parallel, z, z, E_\gamma) \right\}. \tag{2}$$

The expression for the local re-absorption rate obtained from NEGF can also be derived from the rate of power dissipation in an absorbing medium, as given by classical electrodynamics in terms of the imaginary part of the dielectric function $\Im\varepsilon = 2n_r\kappa$ and of the electric field. Inserting the GF based dipole fields with detailed-balance parametrization of the dipole current source provides the generation rate due to re-absorption as follows:

$$\mathcal{R}_{re\text{-}abs}(z, E_\gamma) = \frac{8E_\gamma^4}{\pi\hbar^5 c_0^4} n_r(z, E_\gamma) \kappa(z, E_\gamma) \int dz' \left\{ n_r(z', E_\gamma) \kappa(z', E_\gamma) \right.$$

$$\left. \times f_{BE}[E_\gamma - \Delta\mu_{cv}(z')] \sum_{\mu,\nu} \int \frac{d^2 q_\parallel}{(2\pi)^2} |G_{\mu\nu}(\mathbf{q}_\parallel, z, z', E_\gamma)|^2 \right\}. \tag{3}$$

2.2 Light extraction efficiency

At unit injection efficiency and internal luminescent quantum efficiency *IQE*, the external LED quantum efficiency EQE_{LED} can be written as follows:

$$EQE_{LED} = IQE \cdot \frac{\phi_{out}}{\phi_{int}}, \tag{4}$$

where

$$\phi_{out} = \int dE_\gamma [S_z(z_R, E_\gamma) - S_z(z_L, E_\gamma)] \Big/ E_\gamma \tag{5}$$

is the total photon flux exiting the device as inferred from the normal component S_z of the Poynting vector at the bounding planes of the device ($z = z_{L/R}$), and

$$\phi_{int} = \int dE_\gamma \int dz \, \mathcal{R}_{em}(z, E_\gamma) \tag{6}$$

is the total internally emitted photon flux.

In order to capture the impact of photon recycling on the light out-coupling efficiency, the contributions of re-emission following re-absorption need to be considered. For this purpose, the local modification of the QFLS due to re-absorption has to be iterated, i.e., the contributions to the total light out-coupling due to re-emission of re-absorbed photons are summed until the remaining internal emission falls below a certain threshold. Hence, at each iteration i, the Poynting vector is computed based on the QFLS induced by the re-absorption, which gives the contribution to the total EQE via (4) and (5):

$$EQE_{\text{LED}} = \sum_i [\Delta EQE_{\text{LED}}]^i, \tag{7}$$

$$\left[\Delta EQE_{LED}\right]^i = \frac{\phi_{\text{out}}[\Delta\mu^i]}{\phi_{\text{int}}[\Delta\mu^0]} \tag{8}$$

While an accurate assessment would require full consideration of the charge transport problem, we will here restrict the discussion to the two limiting cases of ideal transport and full charge carrier localization, respectively.

Localized carriers In this case, we neglect the transport of charges generated due to re-absorption and assume that any excess carrier density leads to local re-emission. For each location z in the active layer, the QFLS of two subsequent iteration steps are therefore related via

$$\mathcal{R}_{\text{em}}\left[\{\Delta\mu(z)\}^{i+1}\right](z) = IQE \cdot \mathcal{R}_{\text{re-abs}}\left[\{\Delta\mu(z)\}^i\right](z) \quad \forall z \tag{9}$$

where the local rates for emission and re-absorption are given by the energy integration of Exprs. (2) and (3), and the internal quantum efficiency *IQE* measures the efficiency of the internal photoluminescence process. For a straightforward solution of (9), we use again the Boltzmann approximation to the Bose-Einstein function and rewrite the expressions for the rates as follows:

$$\mathcal{R}_{\text{em}}(z) = \mathcal{M}_{\text{em}}(z)F[\Delta\mu(z)], \tag{10}$$

$$\mathcal{R}_{\text{re-abs}}(z) = \int dz' \mathcal{M}_{\text{re-abs}}(z, z')F[\Delta\mu(z')], \tag{11}$$

$$F[\Delta\mu] \equiv \exp\left[\Delta\mu/(k_{\text{B}}T)\right]. \tag{12}$$

If cast into a spatially discretized form, this provides directly the update of the QFLS:

$$F_k^{i+1} = IQE \cdot \sum_l \left[\mathcal{M}_{\text{re-abs}}\right]_{kl} / \left[\mathcal{M}_{\text{em}}\right]_k F_l^i, \tag{13}$$

where k and l are spatial indices. As the $\mathcal{M}$ coefficient matrices do not depend on the iteration, we have to compute them only once prior to the iteration. The iteration converges when $F^i/F^0 < \eta$ for a threshold parameter $\eta \ll 1$.

Ideal transport In the opposite case, transport within the device is ideal and carriers move with infinite mobility. This corresponds to a spatially constant QFLS $\Delta\mu$[1]. The relation between the rates of re-absorption and (re-)emission becomes a non-local one,

$$\int \mathrm{d}z \, \mathcal{R}_{\mathrm{em}}(z)[\Delta\mu^{i+1}] = IQE \cdot \int \mathrm{d}z \, \mathcal{R}_{\mathrm{re-abs}}(z)[\Delta\mu^{i}], \tag{14}$$

which provides the iteration

$$F[\Delta\mu^{i+1}] = F[\Delta\mu^{i}] \cdot IQE \cdot \bar{\mathcal{M}}_{\mathrm{re-abs}}/\bar{\mathcal{M}}_{\mathrm{em}} \tag{15}$$

where

$$\bar{\mathcal{M}}_{\mathrm{re-abs}} = \int \mathrm{d}z \int \mathrm{d}z' \mathcal{M}_{\mathrm{re-abs}}(z,z'), \quad \bar{\mathcal{M}}_{\mathrm{em}} = \int \mathrm{d}z \, \mathcal{M}_{\mathrm{em}}(z). \tag{16}$$

2.3 Parasitic absorption

While the explicit evaluation of parasitic absorption is not required here for the quantification of the impact of photon recycling on the light extraction efficiency, it can be instructive to analyze parasitic absorption losses in the different layers of the device and to compare the maximum EQE with the value obtained from using the global parasitic absorption (Cho et al. 2020):

$$EQE_{\mathrm{LED}}^{\mathrm{max}}[A_{\mathrm{para}}] = EQE_{\mathrm{LED}}^{(0)}/(EQE_{\mathrm{LED}}^{(0)} + A_{\mathrm{para}}). \tag{17}$$

The parasitic absorption is evaluated by summing the contributions to the re-absorption from the non-active layers, $A_{\mathrm{para}} = \sum_{l} A_{\mathrm{para}}^{l}$ where the individual contribution of layer l is given by

$$A_{\mathrm{para}}^{l} = \phi_{\mathrm{int}}^{-1} \int_{z_{\mathrm{min}}^{l}}^{z_{\mathrm{max}}^{l}} \mathrm{d}z \, \mathcal{R}_{\mathrm{re-abs}}(z). \tag{18}$$

3 Numerical simulation results

The optical modes contributing to the internal emission are analyzed in Fig. 1, which shows the emission rate integrated spatially over the active layer and resolved in energy and in-plane wave vector (normalized to the maximum value of the vacuum wave vector), for the case of a 50 nm metal halide perovskite ($PEA_2Cs_{n-1}Pb_nBr_{3n}$) layer (a) in air and (b) with an aluminum reflector attached at one side[2]. In the absence of the metallic mirror, the emission rate is dominated by guided modes: the dotted lines mark the corresponding solutions to the transcendental eigenmode equation for the perovskite slab (Jackson 1998; Reisinger 1973). On the other hand, the presence of a metallic reflector leads to the

---

[1] Note that we still assume that all of the carriers generated via re-absorption remain in the system and recombine radiatively, i.e., there is no reduction of $\Delta\mu$ due to either, non-radiative recombination or charge carrier extraction.

[2] *nk*-data from Ref. (Cho et al. 2020) (perovskite) and the Setfos material database (Al).
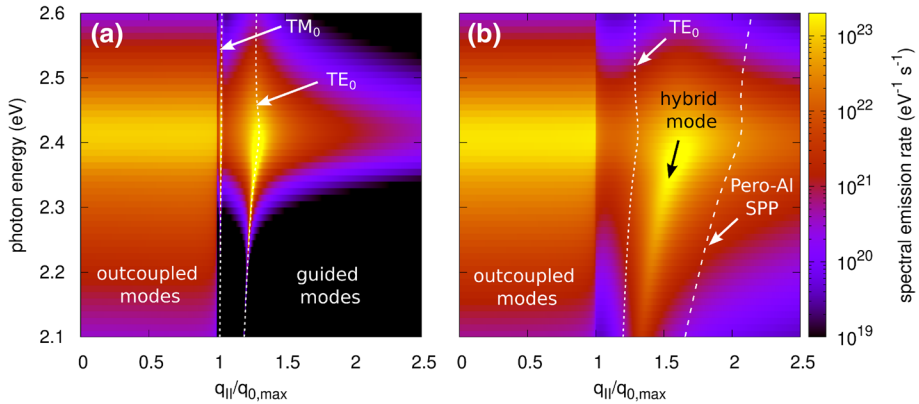
Fig. 1 Analysis of the internal emission rate in a 50 nm metal halide perovskite slab in terms of contributing optical modes, resolved in photon energy and normalized in-plane photon wave vector: **a** In the absence of a metallic reflector, the emission is dominated by guided modes. **b** In the presence of a metallic reflector, the dominant contribution stems from the hybridization of guided modes with surface plasmon polariton modes at the perovskite-metal interface.
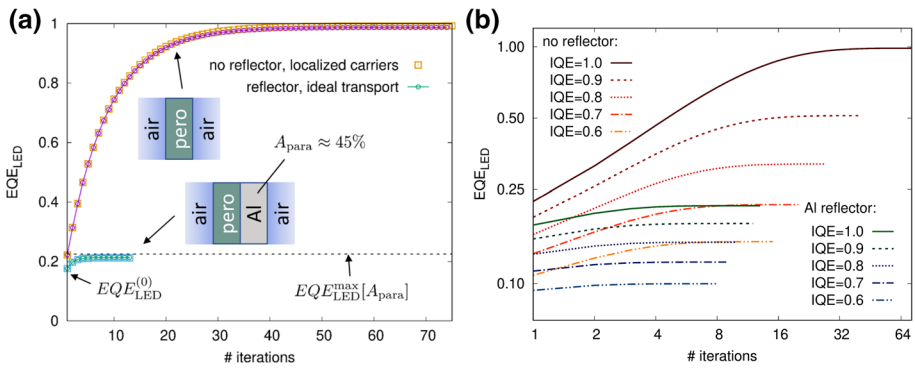

Fig. 2 **a** Evolution of the external LED quantum efficiency of the 50 nm perovskite layer with subsequent contributions from photon re-absorption and re-emission, under the assumption of IQE=1 and ideal transport/flat QFLS (circles) or fully localized charge carriers (squares). While the total (top+bottom) EQE converges to 100% for the perovskite slab in air, parasitic absorption limits the EQE to around 20% for the slab with metallic reflector. **b** For IQE<1, the EQE gain due to photon recycling is reduced substantially, with the reduction being more drastic in the reflector-free case.

hybridization of the guided modes with the surface plasmon polariton (SPP) modes of the perovskite-aluminum interface (Niv et al. 2012), for which the dispersion relation (see, e.g. Haug et al. 2008) is indicated by dashed lines.

The iteration of the external quantum efficiency for the two configurations of Fig. 1 is displayed in Fig. 2a, considering both ideal transport (circles) and fully localized charge carriers (squares) at an IQE of 100%. In this case, the transport regime is found to have only a minor effect on the light out-coupling. In the reflector-free case, the EQE (for overall emission) converges to 100%, as there are no parasitic losses, and eventually, all of the light initially emitted internally will be coupled out. However, since there is no reflector, only
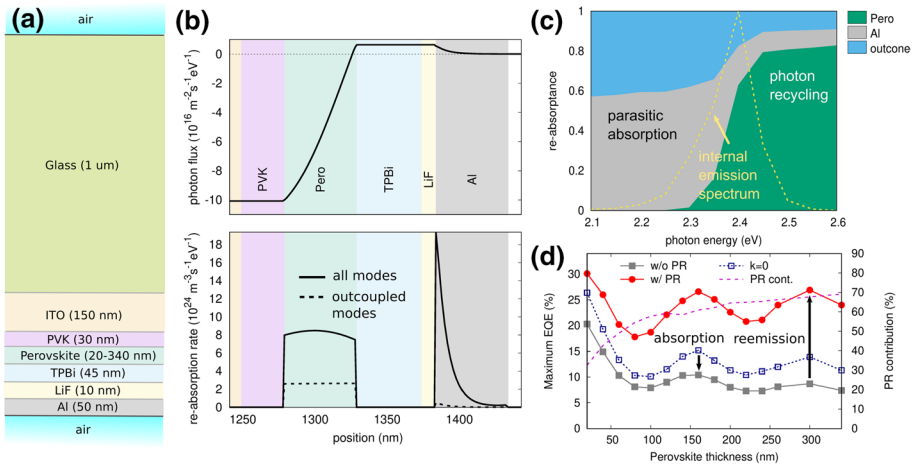
Fig. 3 Analysis of the light propagation, re-absorption and extraction in a realistic PeLED device stack (similar to Ref. Cho et al. (2020)): **a** Device stack layout. **b** Spectral photon flux (upper subfigure) and local re-absorption rate (dashed line: absorption in out-coupled modes). **c** Fraction of the internally emitted photons that are re-absorbed, resolved in energy and by layer. **d** External quantum efficiency of the full stack with and without consideration of PR. The data for vanishing extinction coefficient is obtained from simulation with Setfos.

50% of the light emitted internally will be coupled out to either side. In the presence of an aluminum reflector in contact with the perovskite, on the other hand, parasitic absorption (dashed lines: evaluation of Eq. (17)) amounts to around 45% and photon-recycling leads to an only modest enhancement of the light out-coupling. For lower IQE and ideal transport [Fig. 2b], the EQE enhancement is substantially reduced in both situation, with the absolute reduction being more pronounced for the case without parasitic absorption.

In full PeLED device stacks such as, e.g., those studied in Ref. (Cho et al. 2020), in addition to parasitic losses at metallic reflectors, there can be parasitic absorption in transparent contact layers and light confined to substrate guided modes that both reduce the efficiency of light out-coupling. Figure 3a shows a multilayer device design similar to that of Ref. (Cho et al. 2020). For a perovskite emitter thickness of 50 nm and in the limit of ideal transport and IQE = 1, the photon flux (obtained from the Poynting vector) at a photon energy of $E_\gamma = 2.4$ eV and the corresponding local re-absorption rate are displayed in Fig. 3b, with the contribution of out-coupled modes to the re-absorption indicated by dashed lines. As can be inferred from Fig. 3c showing the energy resolved fraction of internally emitted light that is re-absorbed in a given layer, there are no parasitic losses in the transparent contact layers at the energies of internal emission, but there are still losses related to the electrode in spite of the spatial separation from the emitter layer[3] which are dominated by SPP and hybrid modes outside of the outcone, i.e., with transverse wave vector $q_\parallel > q_0 = E_\gamma/(\hbar c_0)$. There is, however, also significant re-absorption (even in the outcone) by the perovskite itself, which shows in Fig. 3d as a reduction of the EQE without PR (filled squares) from the simulation with vanishing extinction coefficient ($k = 0$, open squares: computed with the opto-electronic device simulation tool |*Setfos*| Fluxim, 2021). If

---

[3] In fact, reduction of contact area was suggested in Ref. (Cho et al. 2020) to increase EQE further.

photon recycling is considered, the assumption of 100% internal quantum efficiency turns the re-absorption into a sizable gain of out-coupling efficiency, which increases with emitter layer thickness. Considering the discrepancies in optical data, numerical models and the details of supporting layers used, the agreement with the result published in Ref. (Cho et al. 2020) (Fig. 3c therein) is remarkable.

Owing to the parametrization of the emission model in terms of the local QFLS, coupling to a drift-diffusion model of charge transport is straight-forward, and will allow to extend the present analysis to a configuration-specific assessment of electrical losses due to carrier leakage and to non-radiative recombination in the bulk and at interfaces (Zeder et al. 2022).

4 Conclusions

We discuss the application to perovskite light emitting devices of a novel modelling framework for photon emission and recycling that is based on a detailed-balance compliant Green's function formalism. The enhancement of the external quantum efficiency due to photon recycling is quantified in limiting transport regimes and for systems with different nature of the dominant modal contribution to the radiative power dissipation, which is evaluated without limitations in resolution owing to the absence of divergence issues. While good agreement is found with the literature in terms of PR-related EQE enhancement at the optical limit, this work paves the way to full opto-electronic optimization of device designs for improved light emission properties.

Data availability All of the material data used in the simulations is available from the authors upon request.

Code availability The code developed for the simulation of photon recycling is closed source. The simulation software Setfos is available commercially and will include the photon recycling model in an upcoming version.

Declarations

Conflict of interest All of the authors are employed at least in part by Fluxim AG that commercializes simulation software for light emitting devices.

References

Aeberhard, U., Rau, U.: Microscopic perspective on photovoltaic reciprocity in ultrathin solar cells. Phys. Rev. Lett. **118**, 247702 (2017). https://doi.org/10.1103/PhysRevLett.118.247702

Aeberhard, U., Zeder, S., Ruhstaller, B.: Reconciliation of dipole emission with detailed balance rates for the simulation of luminescence and photon recycling in perovskite solar cells. Opt. Express **29**(10), 14773–14788 (2021). https://doi.org/10.1364/OE.424091

Cho, C., Greenham, N.C.: Computational study of dipole radiation in re-absorbing perovskite semiconductors for optoelectronics. Adv. Sci. **8**(4), 2003559 (2021). https://doi.org/10.1002/advs.202003559

Cho, C., Zhao, B., Tainter, G.D., Lee, J.Y., Friend, R.H., Di, D., Deschler, F., Greenham, N.C.: The role of photon recycling in perovskite light-emitting diodes. Nat. Commun. **11**, 611 (2020). https://doi.org/10.1038/s41467-020-14401-1

Fluxim AG.: *Setfos v5.2* (2021). https://www.fluxim.com/setfos

Haug, F.J., Söderström, T., Cubero, O., Terrazzoni-Daudrix, V., Ballif, C.: Plasmonic absorption in textured silver back reflectors of thin film solar cells. J. Appl. Phys. **104**, 064509 (2008). https://doi.org/10.1063/1.2981194

Jackson, J.: Classical Electrodynamics. John Wiley & Sons, NewYork (1998)

Niv, A., Gharghi, M., Gladden, C., Miller, O.D., Zhang, X.: Near-field electromagnetic theory for thin solar cells. Phys. Rev. Lett. **109**(13), 138701 (2012). https://doi.org/10.1103/PhysRevLett.109.138701

Paulus, M., Gay-Balmaz, P., Martin, O.J.F.: Accurate and efficient computation of the Green's tensor for stratified media. Phys. Rev. E **62**, 5797 (2000). https://doi.org/10.1103/PhysRevE.62.5797

Reisinger, A.: Characteristics of optical guided modes in lossy waveguides. Appl. Opt. **12**(5), 1015–1025 (1973). https://doi.org/10.1364/AO.12.001015

Stranks, S.D., Snaith, H.J.: Metal-halide perovskites for photovoltaic and light-emitting devices. Nat. Nanotechnol. **10**, 391–402 (2015). https://doi.org/10.1038/nnano.2015.90

Tan, Z.K., Moghaddam, R.S., Lai, M.L., Docampo, P., Higler, R., Deschler, F., Price, M., Sadhanala, A., Pazos, L.M., Credgington, D., Hanusch, F., Bein, T., Snaith, H.J., Friend, R.H.: Bright light-emitting diodes based on organometal halide perovskite. Nat. Nanotechnol. **9**, 687–692 (2014). https://doi.org/10.1038/nnano.2014.149

Zeder, S., Ruhstaller, B., Aeberhard, U.: Assessment of photon recycling in perovskite solar cells by fully coupled optoelectronic simulation. Phys. Rev. Appl. **17**, 014023 (2022). https://doi.org/10.1103/PhysRevApplied.17.014023

Zhang, L., Yang, X., Jiang, Q., Wang, P., Yin, Z., Zhang, X., Tan, H., Yang, Y.M., Wei, M., Sutherland, B.R., Sargent, E.H., You, J.: Ultra-bright and highly efficient inorganic based perovskite light-emitting diodes. Nat. Commun. **8**, 15640 (2017). https://doi.org/10.1038/ncomms15640